Letter

Trisubstituted 1,3,5-Triazines: The First Ligands of the sY12-Binding Pocket on Chemokine CXCL12

Daniel J. Sprague, Anthony E. Getschman, Tyler G. Fenske, Brian F. Volkman, and Brian C. Smith*

Cite This: ACS Med. Chem. Lett. 2021, 12, 1773−1782

Read Online

ACCESS | Metrics & More | Article Recommendations | Supporting Information

ABSTRACT: CXCL12, a CXC-type chemokine, binds its receptor CXCR4, and the resulting signaling cascade is essential during development and subsequently in immune function. Pathologically, the CXCL12−CXCR4 signaling axis is involved in many cancers and inflammatory diseases and thus has sparked continued interest in the development of therapeutics. Small molecules targeting CXCR4 have had mixed results in clinical trials. Alternatively, small molecules targeting the chemokine instead of the receptor provide a largely unexplored space for therapeutic development. Here we report that trisubstituted 1,3,5-triazines are competent ligands for the sY12-binding pocket of CXCL12. The initial hit was optimized to be more synthetically tractable. Fifty unique triazines were synthesized, and the structure−activity relationship was probed. Using computational modeling, we suggest key structural interactions that are responsible for ligand−chemokine binding. The lipophilic ligand efficiency was improved, resulting in more soluble, drug-like molecules with chemical handles for future development and structural studies.

KEYWORDS: CXCL12, chemokines, SDF-1, CXCR4, triazines, sulfotyrosine
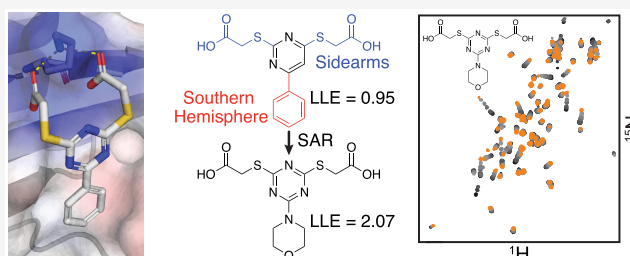
Chemokines are small, chemotactic, proinflammatory proteins.[1] Through G-protein-coupled receptor (GPCR) signaling, chemokines are responsible for physiological processes such as cell trafficking, immune surveillance, organogenesis, angiogenesis, and embryogenesis.[2] Under pathological conditions, this same chemoattractant property implicates chemokines in many diseases, including inflammatory and autoimmune disorders, cardiovascular disease, and cancer. CXCL12 is a constitutively expressed CXC-type chemokine that binds to chemokine receptors CXCR4 and ACKR3 and is essential during embryonic development.[3] After development, the main function of CXCL12 is to mediate the inflammatory response, participate in immune surveillance, and maintain tissue homeostasis by trafficking lymphocytes to tissues such as the lymph nodes, lungs, and bones. Human cancers hijack this process by upregulating chemokine receptors; CXCR4 is upregulated in over 20 human cancers, thereby allowing metastasis to areas of the body producing CXCL12.[4] Small molecules capable of disrupting the CXCL12−CXCR4 signaling axis have demonstrated value,[5] and extensive research has been dedicated to this end, as discussed below.

Traditionally, efforts have been directed at CXCR4 antagonism.[6] However, most clinical trials targeting this GPCR have failed because of toxicity. Though originally halted in Phase II clinical trials for HIV because of cardiotoxicity but now approved for the treatment of non-Hodgkin's lymphoma and multiple myeloma, AMD3100 (Plerixafor) is the only FDA-approved CXCR4 antagonist to date.[7] Recently, the peptide BL-8040 (Motixafortide) entered Phase II clinical trials, demonstrating promise in the treatment of AML[8,9] and pancreatic cancer.[10] Finally, AMD-070, an orally available analogue of Plerixafor, is in Phase III clinical trials[11] for WHIM syndrome.[12] Despite the tremendous clinical potential for inhibiting CXCL12−CXCR4 signaling, the low success rate and potential toxicity of CXCR4-targeting strategies emphasizes the need for alternative strategies to disrupt this signaling pathway.

An alternative solution is to target the chemokine directly instead of the receptor. Through a "two-step, two-site" binding and activation process,[13] CXCL12 is involved in extensive protein−protein interactions (PPIs) with CXCR4, and these interactions provide an attractive avenue for small-molecule development.[14] For example, a chalcone[15] and its derivatives[16] bind CXCL12, prevent CXCR4 activation, and are active in vivo in models of allergic airway diseases and pulmonary hypertension.[17] However, additional structural studies of the binding of these molecules to CXCL12 is needed. Additionally, NOX-A12, a non-orally bioavailable RNA oligonucleotide that neutralizes CXCL12,[18] is in Phase I/II clinical trials for
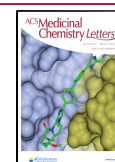
neurological, colorectal, and pancreatic cancer treatment, and NOX-A12 was recently approved for increased dosing and further studies in humans.[19] Nevertheless, there are no approved therapies targeting CXCL12, and a small molecule targeting CXCL12 has yet to enter any human trial.

The initial step in the formation of the active CXCL12–CXCR4 signaling complex is the binding of sulfotyrosine (sY) residues on the extracellular N-terminus of CXCR4 to the conserved core of CXCL12. CXCL12 has three unique "hot spots" for binding of sY residues on CXCR4: sY7, sY12, and sY21.[20] Of these, the interactions between CXCL12 and sY12 and sY21 of CXCR4 are responsible for most of the binding energy of the complex and confer most of the specificity of the interaction. Therefore, small molecules that bind in these sY-binding pockets are predicted to interrupt the CXCL12–CXCR4 signaling axis by inhibiting the initial formation of the complex.

In 2010, we demonstrated this proof of principle using a structure-based *in silico*/NMR approach leading to a small molecule that bound to CXCL12.[21] Lead optimization resulted in a set of tetrazole-containing compounds that bind with micromolar affinity to the sY21 binding pocket of CXCL12 and interrupt CXCL12–CXCR4-mediated chemotaxis *in vitro*.[20]

Achieving this success led us to more broadly investigate the feasibility of individually targeting each of the sY binding sites, resulting in the identification of compound **1** (Table 1)

Table 1. Initial SAR by Catalog
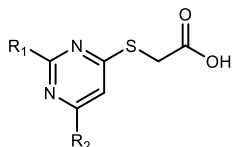
compound	R_1	R_2	K_d (μM)[a]
1	−SCH$_2$CO$_2$H	−Ph	169 ± 12
2	−SCH$_2$CO$_2$H	−CH$_3$	~1200
3	−H	−Ph	~900
4	−H	−CH$_3$	NB

[a]NB = nonbinder.

through *in silico* screening of the ZINC library.[22] Compound **1** binds the sY12 pocket of CXCL12.[23,24] Here we investigated the structure–activity relationships (SARs) of **1** with the goal of decreasing the lipophilicity while maintaining or increasing the potency. We anticipate that these studies will enable future fragment-linking campaigns with fragments that bind adjacent sY-binding pockets on CXCL12 to discover novel and potent CXCL12-targeting inhibitors.

To determine the binding affinity of the molecules to CXCL12, we employed 2D NMR spectroscopy to monitor chemical shift perturbations of amino acid residues residing in the sY12 binding pocket upon compound binding (Figure 1A). Prior studies in the laboratory[23,24] indicated that upon small-molecule binding to the sY12 pocket, the residues consistently demonstrating the largest and most specific shifts are I28, V39, and A40 (Figure 1B). Affinity was determined by nonlinear regression of the chemical shift perturbations plotted over a titratable range of concentrations (Figure 1C).[25] Because the overarching goal of the study was to develop a highly soluble molecule with potent binding to the sY12 binding pocket of

CXCL12, only compounds that were soluble to ≥1600 μM and induced a chemical shift perturbation of ≥0.5 ppm in at least two of the three residues (I28, V39, and A40) were labeled as "binders".

Initially we performed a brief SAR by catalog to investigate which features of **1** are important for interactions with CXCL12 (Table 1). Replacing the phenyl group with a methyl group (**2**) decreased the binding affinity about 7-fold (Table 1). Removing the thioglycolic acid moiety from the 2-position of the pyrimidine (**3**) also decreased binding to CXCL12, resulting in a K_d of about 900 μM—a 5-fold decrease from the parent molecule (Table 1). Finally, replacing the phenyl group with a methyl group at the 4-position and simultaneously removing the thioglycolate substituent at the 2-position (**4**) abolished binding to CXCL12 (Table 1). This suggests that the hydrophobic 4-position and the two carboxylic acids work synergistically to bind the sY12 site of CXCL12. With this knowledge, we further investigated this scaffold to delineate important characteristics for binding *via* SAR and ultimately to develop more soluble and potent small molecules with favorable characteristics for future fragment linking.

Improving the simplicity of the synthesis of the target compounds was imperative to our ability to rapidly generate a library of compounds. Therefore, we began by transforming the asymmetrical pyrimidine ring on **1** into the symmetrical 1,3,5-triazine, resulting in **5** (Figure 2). The ring alteration had no effect on binding of the molecule to CXCL12 (158 ± 66 μM for **5** vs 169 ± 12 μM for **1**; Figures 2 and S1). While maintaining binding, this scaffold increased the ease of synthesis by creating a symmetric molecule and allowed inexpensive, commercially available cyanuric chloride to be used as a starting material for many of the analogues. The triazine also imparts increased polarity and hydrophilicity to the molecule, thereby improving the drug-like characteristics. These improvements led us to maintain the triazine scaffold throughout the rest of our investigation. The triazine was then divided into two modular sections for SAR studies: (1) the side arms of the northern hemisphere and (2) the characteristics of the southern hemisphere attached to the triazine (Figure 2).

We began by investigating various side-arm substitutions. These analogues (**5**, **7**, and **9a−m**) were readily accessible from commercially available 2,6-dichloro-4-phenyl-1,3,5-triazine (**6**) *via* nucleophilic aromatic substitution by refluxing in the presence of the appropriate nucleophile (Scheme 1). First, we replaced the thioglycolate side arm with glycine, resulting in **9a**, which retained binding affinity to CXCL12 (Table 2, entry 2, and Figure S2). This S-to-N substitution allowed us to use readily available (and less noxious) amino acids in our SAR studies. We then turned to the other functional group on the side arm—the carboxylic acid moiety—to investigate its role in binding to CXCL12. Hypothesizing that the acid is necessary for creating a salt bridge, we blocked the free acid as a *tert*-butyl ester (**7**) and as a ketone (**9b**). These changes destroyed binding of the compound to CXCL12 (Table 2, entries 3 and 4). Next, we probed the effect of lengthening the side arm. We first synthesized **9c** as a homologated variant of **5**. The homologation had no effect on binding, as **9c** had a nearly identical affinity of 158 ± 73 μM (Table 2, entry 5, and Figure S3). However, there was a limit on the tolerable distance between the triazine core and the acid. This was apparent because homologating **9c** by one carbon afforded **9d**, which did not bind CXCL12 (Table 2, entry 6). Compound **9e**, the
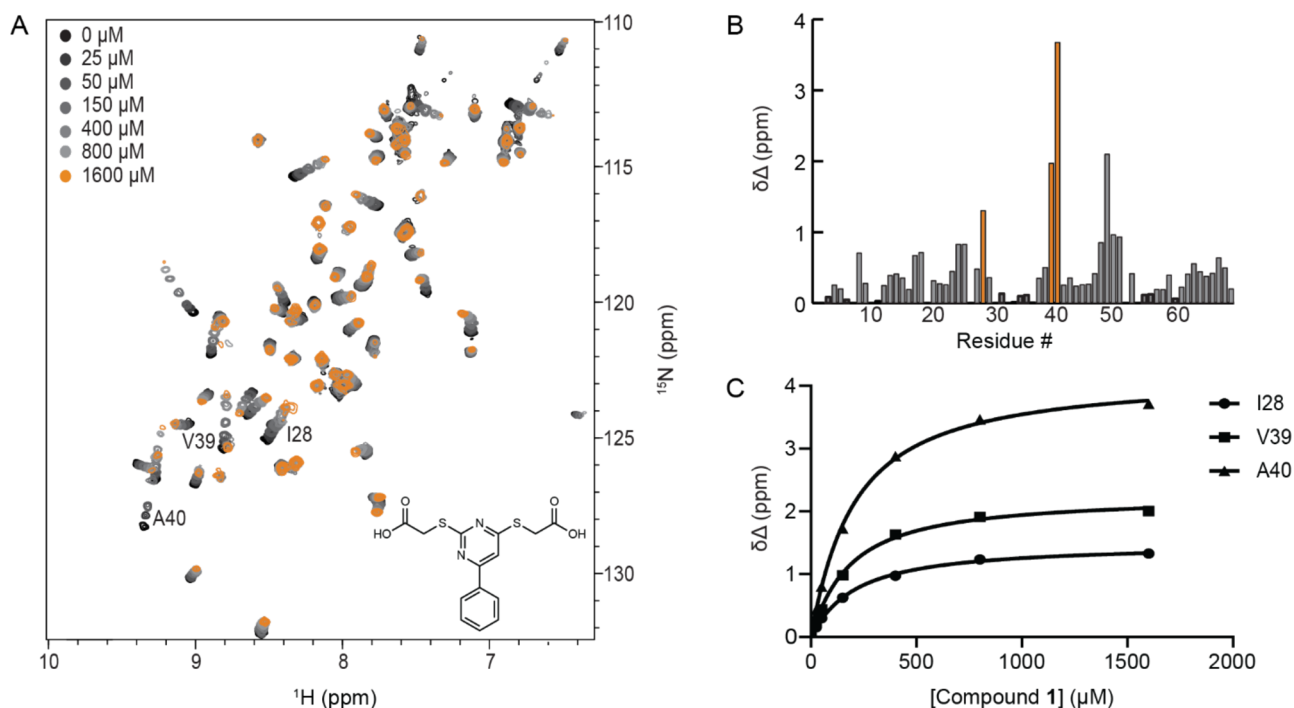
Figure 1. Data from titration of CXCL12 with compound **1**. (A) HSQC spectrum of CXCL12 upon titration with increasing concentrations of **1**. (B) Depiction of the maximal chemical shift perturbation of CXCL12 residues upon binding of **1** at 1600 μM. Residues I28, V39, and A40 are highlighted in orange. (C) Titration curves for binding of **1** to CXCL12.
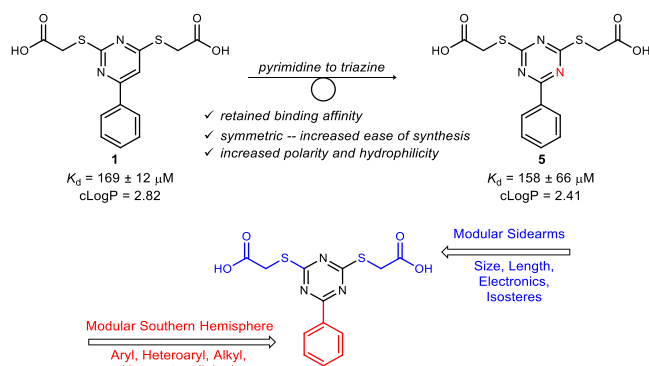

Figure 2. Replacing the pyrimidine ring with a triazine ring retains the binding properties.

amino variant of **9d**, also displayed no binding (Table 2, entry 7).

Interested in whether steric bulk at the α-carbon would be tolerated in the setting of a constant distance between the triazine and the acid, we synthesized L-norleucine-derived triazine **9f**, which bound with K_d = 156 ± 76 μM (Table 2, entry 8), demonstrating that indeed, substitution at the α-carbon actually improved the binding ~2-fold compared with **9a**. Interestingly, **9g**, the enantiomer of **9f**, still bound to CXCL12 (Table 2, entry 9), suggesting that the *n*-butyl side chains of norleucine are largely oriented outside the critical interactions within the binding pocket.

Finally, we examined whether carboxylic acid isosteres with varying pK_a or hydrogen-bonding ability would bind as effectively. Amide **9h**, trifluoromethyl-substituted alcohol **9i**, and alcohol **9j** are all capable of donating a hydrogen bond. However, none of them bound CXCL12 (Table 2, entries 10−12). To investigate different acidities, we synthesized

hydroxamic acid **9k** ($pK_a \sim 8−10$) and sulfonic acid **9l** ($pK_a \sim −2$), and we synthesized benzoic acid **9m** as a structural variant of the necessary carboxylic acid side chain. Compounds **9k** and **9l** did not demonstrate binding (Table 2, entries 13 and 14). Compound **9m** caused aggregation and precipitation of the protein, revealing no spectra upon acquisition (Table 2, entry 15).

These results suggest that specifically the carboxylic acid moiety is critical for CXCL12 binding affinity. For structural insight into the observed specificity, we turned to computational docking. *In silico* docking using Glide generated 10 000 potential low-energy binding poses for the interaction of **5** with CXCL12. These poses were filtered using experimental constraints by predicting the chemical shift perturbation for each pose and correlating the predicted chemical shift perturbations to the experimental ones.[26] These top-performing filtered poses suggest that a salt bridge is formed between K27 and the carboxylic acid side arm of **5**, consistent with the carboxylate moiety being necessary for efficient binding (Figure 3). Compounds not able to form a salt bridge with lysine do not show any binding to the sY12 pocket of CXCL12. One exception to this is sulfonic acid **9l**, which can readily form an ion pair.

Closer inspection of our model of **5** bound to CXCL12 revealed that both carboxylate arms are attracted inward to the lysine, providing a bidentate interaction to hold the compound in the pocket. This presumably occurs *via* a hydrogen-bonding interaction of one carboxylate with the ion pair formed between the other carboxylate and lysine. The necessity of this bidentate interaction is suggested in the initial SAR by the fact that **3**, containing a single side arm, demonstrated >5-fold weaker binding to CXCL12 (Table 1). Pike *et al.* demonstrated that the carboxylate anion is one of the strongest hydrogen-bond acceptors known, whereas sulfate and organosulfonates

Scheme 1. Synthesis of Triazines with Various Side Arms
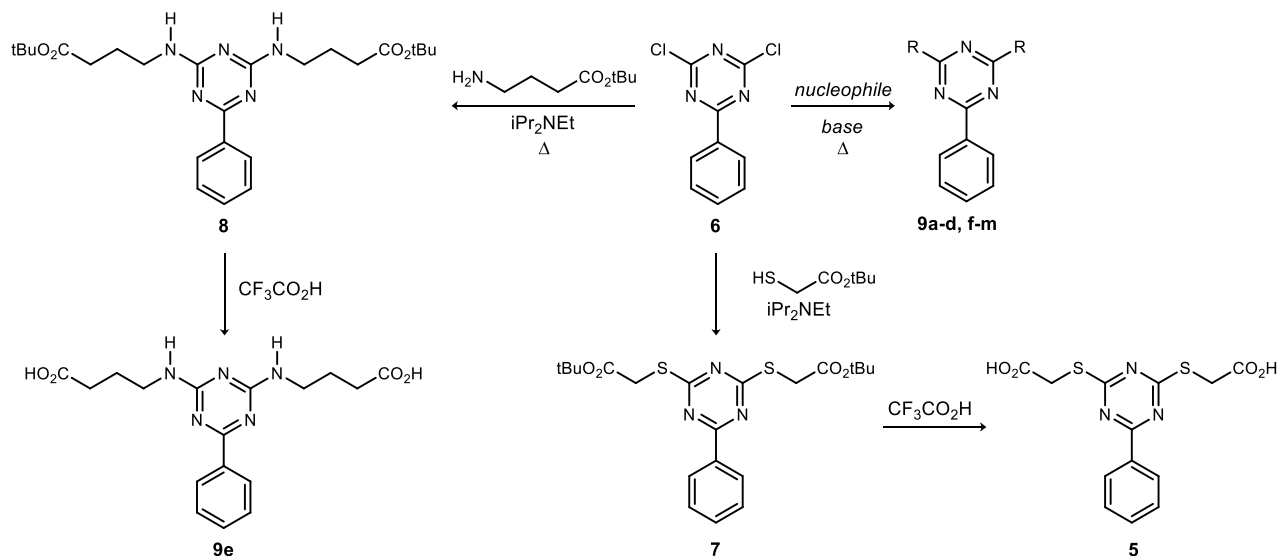
are much weaker hydrogen-bond acceptors, regardless of the countercation.[27] If the extra binding energy from the secondary hydrogen-bonding interaction with K27 is needed for efficient binding, then it is feasible that although sulfonic acid 9l may form a salt bridge, it does not have sufficient hydrogen-bond-acceptor ability to create the bidentate interaction needed to bind in the sY12 pocket of CXCL12. Additionally, the binding is hindered since the salt bridge is likely to be weaker than a carboxylate−ammonium complex because of the noncoordinating nature of an alkylsulfonic acid, necessitating less of a need for the ion pair in solution. Indeed, experiments on docking of 9l to CXCL12 failed to reveal a binding pose demonstrating bidentate interactions in the sY12 pocket. Because of the "Goldilocks effect"[28] afforded by the acidity and hydrogen-bonding properties of 5, the 2-thioglycolic acid moiety was chosen as the side arm to further study the SAR of the triazines.

Next, we investigated important features of the southern hemisphere. We divided these compounds into three groups: triazines containing (1) a 4-aryl or 4-heteroaryl substitution, (2) a 4-alkyl or 4-alkenyl substitution, or (3) a southern hemisphere linked to the triazine *via* a heteroatom bond.

Synthesis of the aryl and heteroaryl analogues started with cheap, commercially available cyanuric chloride (10) (Scheme 2). By careful control of the temperature, nucleophilic aromatic substitution using *tert*-butyl thioglycolate cleanly afforded disubstituted triazine 11 in 82% yield on a gram scale. Under microwave conditions, Pd(PPh$_3$)$_4$-catalyzed coupling of 11 with commercially available boronic acids afforded biaryl products 12a−q. After flash purification, trifluoroacetic acid-mediated deprotection of the *tert*-butyl esters afforded the desired bisacids 13a−q in quantitative yield. We carried the esters through the synthesis instead of the free acids to facilitate purification of the compounds away from impurities after the Suzuki coupling. While ethyl thioglycolate is less expensive than *tert*-butyl thioglycolate and is typically used for similar intermediates, we found difficulties in reproducibility of ester hydrolysis and in isolation of clean bisacids. The *tert*-butyl ester circumvented this problem, and the final step became a simple procedure where the bisesters were treated with
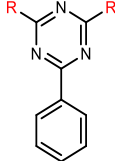
trifluoroacetic acid, and then removal of solvent and excess acid *in vacuo* provided clean product.

Synthesis of triazines bearing alkyl southern hemispheres was accomplished *via* three different methods (Scheme 3). 15 was synthesized in three steps from cyanuric chloride. First, nucleophilic aromatic substitution of cyanuric chloride with benzylmagnesium bromide afforded 2,6-dichloro-4-benzyl-1,3,5-triazine (14). Subsequent microwave-mediated nucleophilic aromatic substitution with thioglycolic acid afforded 15. Despite few reports of adamantyl-group cross-couplings to triazines in the literature, 4-adamantyl-substituted triazine 16 was synthesized in good yield from 2-adamantylzinc bromide and 11 using a variation on a previously published Negishi coupling.[29] As before, simple ester deprotection afforded 17. We attempted to synthesize hexyl-substituted triazine 18 in the same fashion as 14 using hexylmagnesium bromide. However, we were unable to control the substitution to efficiently isolate the desired product. Unsurprisingly, attempting to install the hexyl group *via* S$_N$Ar on 11 resulted in addition to the ester. Using elegant conditions developed by Fürstner and co-workers,[30] we successfully synthesized 18 in excellent yield. Simple deprotection of the esters afforded 19. Alkenyl compound 20 was synthesized *via* sp^2−sp^2 Suzuki coupling in good yield using the pinacol ester of cyclohexenylboronic acid followed by deprotection.

Scheme 4 depicts our strategy to synthesize compounds 24a−l, which have the southern hemisphere linked to the triazine *via* a heteroatom. Two different routes were used. For 24a−f and 24i−k, cyanuric chloride underwent nucleophilic aromatic substitution to afford the 2,6-dichloro-4-substituted triazines 22a−f and 22i−k. These were then treated with *tert*-butyl thioglycolate to afford bisesters 23a−f and 23i−k. As before, acid-mediated deprotection afforded the final bisacids. For 24g, 24h, and 24l, the synthesis began with the common intermediate 11. S$_N$Ar of 11 with the appropriate nucleophiles afforded the fully substituted triazines, which then were treated with acid to afford the final products.

With the library of southern hemisphere variants in hand, we investigated their binding affinity toward CXCL12, beginning with the biaryl systems. We soon learned that adding bulk to the original phenyl ring is not tolerated, as 1-naphthyl-, 2-

Table 2. SAR of Various Side Arms on the Triazine

Entry	R		K_d (µM)[a,b]
1	S—CH₂COOH	5	158 ± 66
2	N—CH₂COOH	9a	355 ± 89
3	S—CH₂C(O)OtBu	7	NB
4	N—CH₂C(O)CH₃	9b	NB
5	S—CH₂CH₂COOH	9c	158 ± 73
6	S—CH₂CH₂CH₂COOH	9d	NB
7	N—CH₂CH₂CH₂COOH	9e	NB
8	9f	9f	156 ± 76
9	9g	9g	383 ± 199
10	N—CH₂C(O)NH₂	9h	NB
11	N—CH(OH)CF₃	9i	NB
12	N—CH₂CH₂OH	9j	NB
13	N—CH₂C(O)NHOH	9k	NB
14	N—CH₂SO₂OH	9l	NB
15	N—C₆H₄COOH	9m	Insoluble

[a]NB = nonbinder. [b]**9m** caused CXCL12 to precipitate.

Figure 3. *In silico* modeling. A predicted low-energy binding pose of **5** in the sY12 pocket is shown with both carboxylate arms chelating the side-chain amino group of K27 and the nonpolar phenyl ring extending toward the sY21 binding pocket.

with K_d = 306 ± 128 µM and demonstrated qualitatively greater solubility when samples were prepared for titration, again demonstrating that electron-rich southern hemispheres are tolerated (Table 3, entry 10, and Figure S5). Triazine **13j** containing a phenol southern hemisphere demonstrated an order of magnitude loss of binding (Table 3, entry 11). Notably, introducing a carboxylic acid in the southern hemisphere (**13k**) afforded a triazine that bound with a K_d value of 133 ± 12 µM (Table 3, entry 12, and Figure S6). This functional group increases the polarity and hydrophilicity of the southern hemisphere and provides a handle for future molecule development.

Next, we investigated heteroaromatic southern hemispheres. Isoquinoline **13l** (Table 3, entry 13) and phenyl ether **13m** (Table 3, entry 14) precipitated the protein from solution. There was a noticeable difference between a furan or thiophene ring as the southern hemisphere. 3-Furyl-substituted triazine **13n** (Table 3, entry 15) precipitated the protein from solution, and 2-furyl-substituted triazine **13o** did not demonstrate binding to CXCL12 (Table 3, entry 16). In contrast, 3- and 2-substituted thienyltriazines **13p** and **13q** were competent ligands for CXCL12, albeit with weakened affinity (Table 3, entries 17 and 18). While the exact reason for the discrepancy between the binding of the furyl- and thienyl-substituted triazines is not readily apparent, it may be attributable to hydrogen-bond-acceptor ability. Both furan and thiophene are electron-rich heterocycles, but sulfur does not appreciably hydrogen-bond. The oxygen within the furan ring can accept a hydrogen bond. Therefore, the furan ring may engage in a disfavorable interaction within the pocket that disrupts its ability to bind, whereas thiophene does not have this issue. Nevertheless, further studies are needed to definitively answer this question.

These results suggest that there is a defined pocket in which the southern hemisphere sits when bound in the sY12 pocket. The fact that increasing the bulk of the southern hemisphere *via* multiple structures abolished ligand binding to CXCL12 supports this, as does our docking model (Figure 3). The data

naphthyl-, anthracenyl-, and mesityl-substituted triazines (**13a–d**) did not demonstrate significant binding in the sY12 pocket (Table 3, entries 2–5). Biphenyltriazine **13e** did demonstrate minimal binding in the sY12 pocket, but unsurprisingly, the compound was insoluble, and a full titration was not feasible (Table 3, entry 6).

Electron-deficient southern hemispheres showed decreased binding affinity, as pentafluorophenyl-substituted triazine **13f** did not demonstrate binding to CXCL12 (Table 3, entry 7). 3,5-Bis(trifluoromethyl)phenyltriazine **13g** bound to CXCL12 but with weaker affinity (Table 3, entry 8). Conversely, electron-rich southern hemispheres were well-tolerated, as demonstrated by anisole-substituted triazine **13h** with K_d = 357 ± 101 µM (Table 3, entry 9, and Figure S4). To increase the hydrophilicity of the molecule, we synthesized **13i** containing a morpholine ring at the 4-position of the phenyl ring. This compound bound comparably to the parent triazine
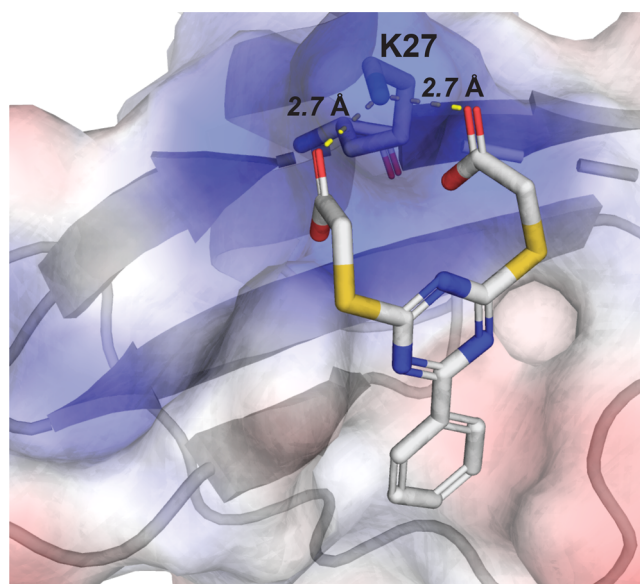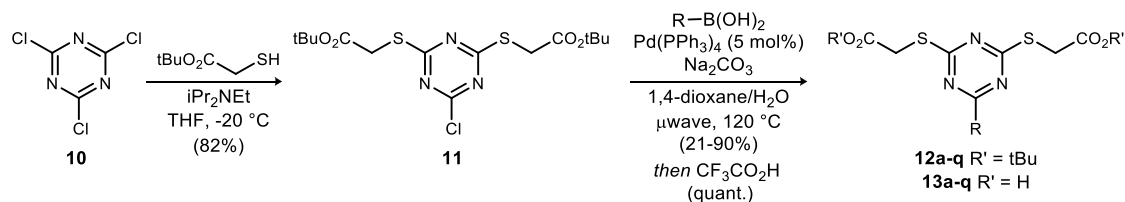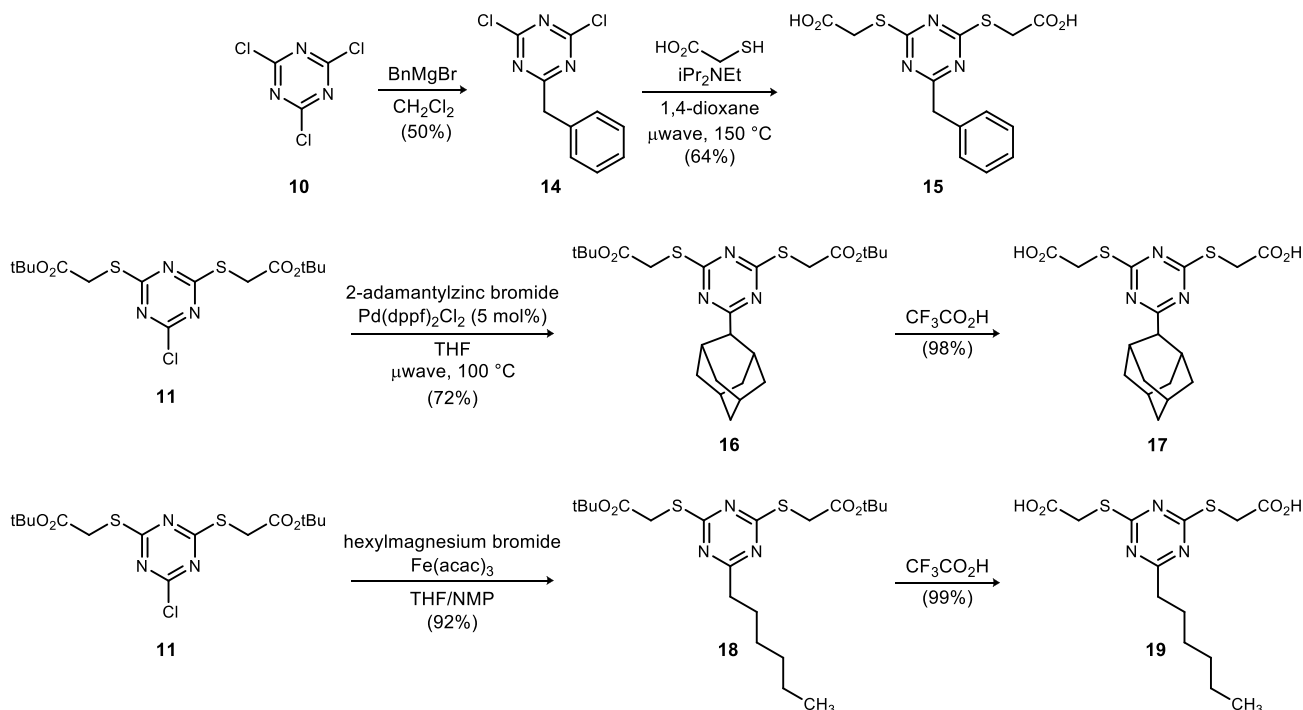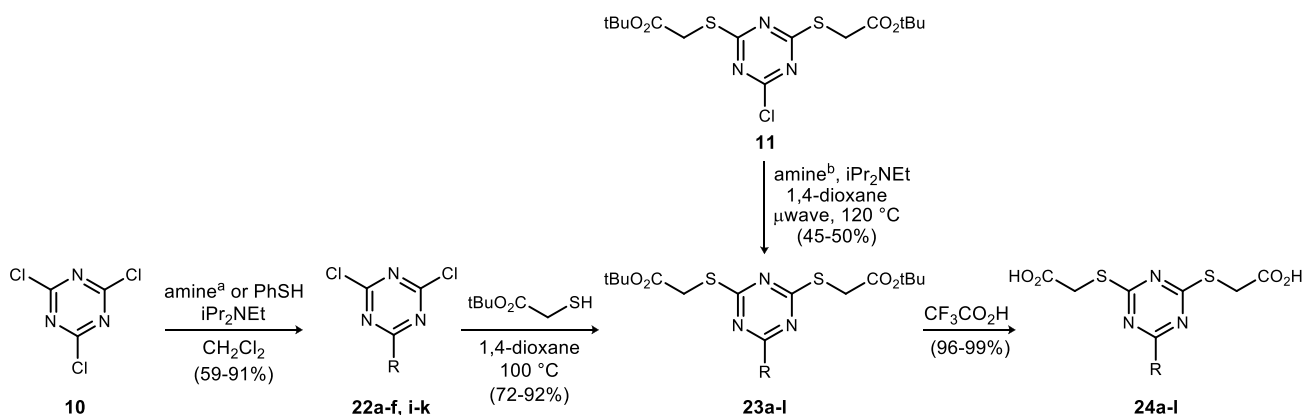
Scheme 2. Synthesis of Triazines Containing Aryl Southern Hemispheres

Scheme 3. Synthesis of Triazines Containing Alkyl Southern Hemispheres

**Scheme 4. Synthesis of Triazines Containing 4-Heteroatom-Linked Southern Hemispheres**

[a]Aniline, 1-bicyclo[1.1.1]pentylamine, cyclohexylamine, dicyclohexylamine, benzylamine, pyrrolidine, or 8-oxa-3-azabicyclo[3.2.1]octane. [b]2-Picolylamine, 3-picolylamine, or N-methylmorpholine.

also suggest that prominent cation−π interactions are present in the binding pocket. Many proteins participate in cation−π interactions as part of their secondary and tertiary structure,[31,32] and small-molecule inhibitors have been designed to take advantage of these interactions for binding to their target.[33] Arginine[34,35] and lysine[31,36] residues are typically most important to these interactions, and multiple positively charged residues are in proximity to the sY12

binding pocket. Further supporting this notion is the observation that electron-deficient southern hemispheres, which have decreased ability to participate in cation−π interactions, bind either weakly or not at all.

Triazines with alkyl southern hemispheres did not yield molecules that bind to CXCL12 (Table 4). This lack of binding is most likely due to the inability of these compounds to participate in cation−π interactions within the sY12 pocket.

Table 3. SAR of Various Aryl Southern Hemispheres
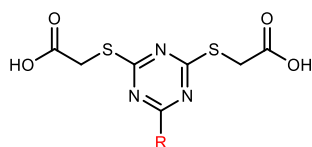
entry	R	compd	K_d $(\mu M)^{a,b}$
1	C_6H_5	5	158 ± 66
2	1-naphthyl	13a	NB
3	2-naphthyl	13b	NB
4	9-anthracenyl	13c	NB
5	mesityl	13d	NB
6	4-Ph-C_6H_4	13e	insoluble
7	C_6F_5	13f	NB
8	3,5-$(CF_3)_2$-C_6H_3	13g	646 ± 23
9	4-MeO-C_6H_4	13h	357 ± 101
10	4-morpholino-C_6H_4	13i	306 ± 128
11	3-OH-C_6H_4	13j	1798 ± 218
12	3-CO_2H-C_6H_4	13k	133 ± 12
13	4-isoquinolyl	13l	insoluble
14	4-PhO-C_6H_4	13m	insoluble
15	3-furyl	13n	insoluble
16	2-furyl	13o	NB
17	3-thiophene	13p	1344 ± 376
18	2-thiophene	13q	1640 ± 190

[a]NB = nonbinder. [b]13e has low solubility. 13l, 13m, and 13n caused CXCL12 to precipitate.

Table 4. SAR of Alkyl Southern Hemispheres
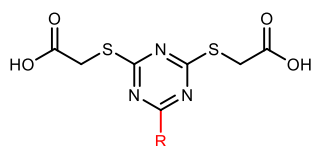
| Entry	R		K_d $(\mu M)^{a,b}$
1	Benzyl	15	NB
2	2-Adamantyl	17	NB
3	[n]Hexyl	19	NB
4		20	Insoluble
5	H	21	NB

[a]NB = nonbinder. [b]20 caused CXCL12 to precipitate

Benzyltriazine 15 shows specific binding to the sY12 pocket (Table 4, entry 1). However, the chemical shift perturbation did not cross our threshold for binding as described above. Adamantyl- and hexyl-substituted triazines (17 and 19, respectively) did not bind to CXCL12 (Table 4, entries 2 and 3). Alkenyltriazine 20 caused the protein to precipitate from solution (Table 4, entry 4). Removing the southern hemisphere altogether in compound 21 also afforded a nonbinding molecule (Table 4, entry 5).

The final group of southern hemispheres we investigated were those attached to the triazine *via* a heteroatom. Creating a thioether by replacing the phenyl group of 5 with a thiophenyl

ring afforded 24a, which demonstrated excellent binding to CXCL12 with K_d = 80 ± 18 μM (Table 5, entry 1, and Figure

Table 5. SAR of 4-Heteroatom-Linked Southern Hemispheres
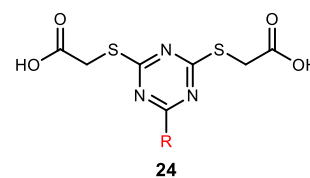
Entry	R	24	K_d $(\mu M)^a$
1	Thiophenyl	24a	80 ± 18
2	Aniline	24b	251 ± 99
3		24c	1355 ± 194
4	$CyNH_2$	24d	170 ± 44
5	Cy_2NH	24e	NB
6	$BnNH_2$	24f	NB
7	3-Picolylamine	24g	NB
8	4-Picolylamine	24h	NB
9	Pyrrolidine	24i	1030 ± 474
10	Morpholine	24j	234 ± 4
11		24k	233 ± 34
12	N-Me-Morpholine	24l	3024 ± 662

[a]NB = nonbinder.

S7). Swapping the phenyl group for an aniline (24b) maintained the binding affinity while increasing the polarity (Table 5, entry 2, and Figure S8). Interestingly, bicyclopentyl-amine 24c bound with a K_d that was an order of magnitude less than that of the parent molecule, even though bicyclopentane is a common isostere of a phenyl ring[37] (Table 5, entry 3, and Figure S9). As above, steric bulk plays a role in fitting within the discrete pocket, and thus, (cyclohexylamino)triazine 24d (Table 5, entry 4, and Figure S10) binds with K_d = 170 ± 44 μM, but (dicyclohexylamino)triazine 24e (Table 5, entry 5) does not bind to CXCL12.

Creating a positively charged molecule by using N-methylmorpholine as opposed to morpholine as the southern amine resulted in a molecule with very weak binding. Our hope was to create a molecule that would be extremely soluble to circumvent solubility issues. Unfortunately, adding the methyl group to 24j, affording 24l, increased the K_d value from 234 ± 4 μM (Table 5, entry 10) to 3024 ± 626 μM (Table 5, entry 12). We attribute this to a combination of positively charged electrostatic repulsion and increased steric bulk.

Overall, linking the southern hemisphere *via* an amine appears to be well-tolerated (Table 5), and in doing so
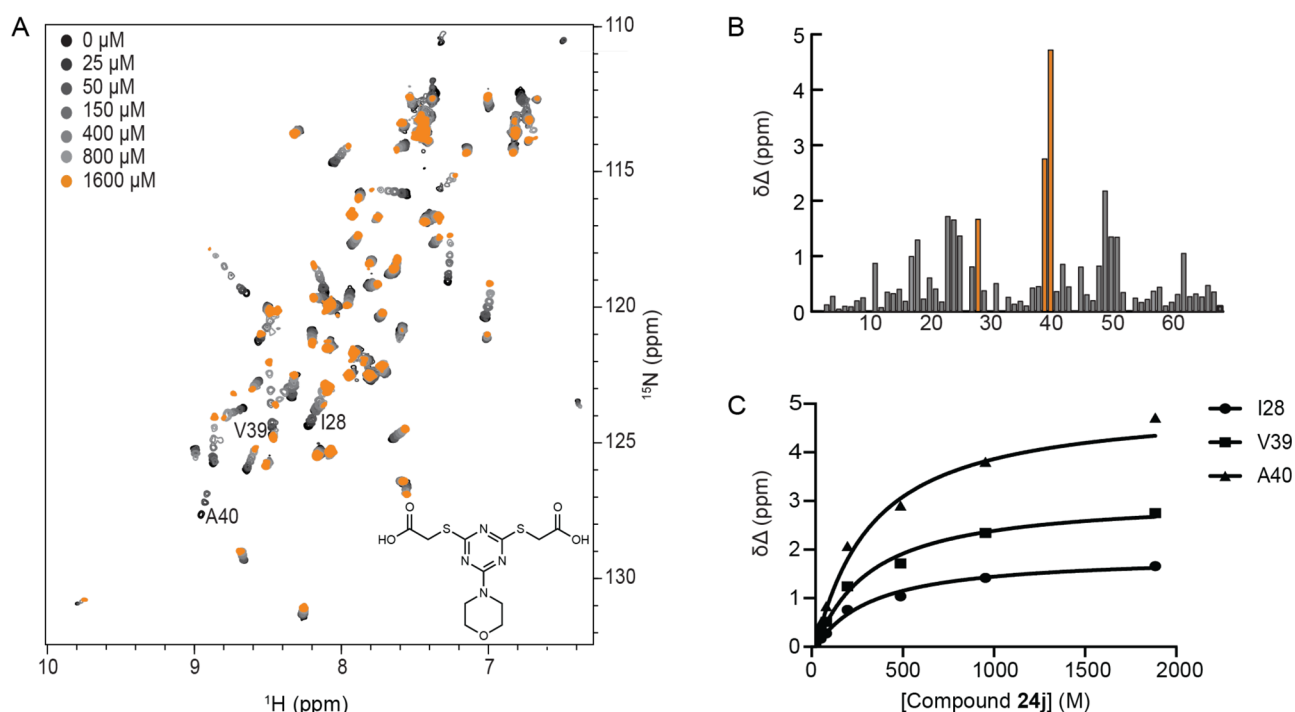
Figure 4. 4-Morpholinotriazine **24j** maintains binding to the sY12 pocket. (A) HSQC spectrum of CXCL12 upon titration with increasing concentrations of compound **24j**. (B) Depiction of the maximal chemical shift perturbation of CXCL12 residues upon binding of compound **24j** at 1600 μM. Residues I28, V39, and A40 are highlighted. (C) Titration curves for binding of compound **24j** to CXCL12.

hydrophilicity and polarity are increased in the molecule. While there is not yet a straightforward rationale for the ability of alkylamine southern hemispheres to bind well in the sY12 pocket of CXCL12, NMR data clearly demonstrate binding in the same pocket as the triazines possessing the aryl southern hemispheres reported above (Figure 4). Although these molecules cannot participate in a cation−π interaction as the aryl southern hemispheres can, there is the possibility of a hydrophobic interaction between the alkyl carbons on the substituent and the residues in the pocket. There is also the possibility that there is an electrostatic interaction between the nitrogen at the 4-position of the triazine and residues within the pocket; however, more structural studies are needed. Regardless, the plethora of commercially available amines allows for a nearly endless number of southern hemispheres to be synthesized in future SAR studies.

On the basis of the complete set of results of our SAR studies, the modularity of the triazine scaffold notably allowed us to increase the lipophilic ligand efficiency (LLE)[38] without sacrificing binding affinity to CXCL12 (Table 6).[39] As stated earlier, increasing the ease of library synthesis by changing our scaffold from pyrimidine **1** to triazine **5** resulted in essentially unchanged binding affinity while simultaneously increasing the

solubility and LLE (Table 6, entries 1 and 3). While compound **24a** demonstrated excellent affinity compared with the rest of our series, this compound is quite lipophilic and qualitatively was not as soluble as some of our other analogues (Table 6, entry 2). It also does not have a chemical handle for future transformations. Because it lacks desirable characteristics in both categories, we decided against carrying **24a** forward for development. Adding a carboxylate arm to the southern hemisphere (**13k**) improved the LLE to 2.06 (Table 6, entry 4). Finally, we realized maximal optimization of the LLE in this study using **24j** (Table 6, entry 5); qualitatively, this molecule was notably more soluble than its analogues as well. Ultimately, we have chosen to carry forward **13k** and **24j** in future studies. The carboxylic acid in the southern hemisphere of **13k** provides a synthetic handle for future derivatization, and there are commercially available analogues of morpholine **24j** that can be explored for further derivatizations. Compound **24k** from this study is one example.

In conclusion, we synthesized 50 trisubstituted 1,3,5-triazines as the first reported ligands of the sY12 pocket of CXCL12. Using a combination of NMR chemical shift perturbation measurements and computational modeling, we probed the structure−activity relationships of the triazine that are necessary for binding to the sY12 pocket on the chemokine. In this family of molecules, carboxylic acid substituents at the 2- and 6-positions of the triazine are necessary to maintain binding affinity. Modeling suggests that these carboxylic acids interact with K27 to promote binding in the CXCL12 pocket. Provided that the molecule is soluble and not bulky, the southern hemisphere modification shows tolerance to aryl and amine modifications. Cation−π interactions may play a role in the interaction of aryl groups with CXCL12; more structural studies are necessary to

Table 6. Demonstration of Improved Lipophilic Ligand Efficiency

entry	compd	K_d (μM)	LE[a]	cLogP	LLE[b]
1	**1**	169 ± 12	0.23	2.82	0.95
2	**24a**	80 ± 18	0.24	3.05	1.05
3	**5**	158 ± 66	0.24	2.41	1.39
4	**13k**	133 ± 12	0.21	1.82	2.06
5	**24j**	234 ± 4	0.23	1.56	2.07

[a]LE = ligand efficiency. [b]LLE = lipophilic ligand efficiency.

determine the interactions that the amine southern hemispheres have with CXCL12.

The necessity of increasing the hydrophilicity during future compound optimization will be important, as many of the compounds screened were either insoluble or precipitated the protein when added. Thus, the molecules that we decided were optimal to carry forward for further development had increased hydrophilicity compared with the starting material along with adequate affinity for the sY12 pocket. They were designed to increase the lipophilic ligand efficiency and to introduce functional handles that can be used for growth of the molecule in the future. Further structural studies are underway to increase our understanding of the binding of these triazines to CXCL12. The results of these X-ray crystallography, NMR spectroscopy, and docking experiments will be reported in due course.

ASSOCIATED CONTENT

Supporting Information

The Supporting Information is available free of charge at https://pubs.acs.org/doi/10.1021/acsmedchemlett.1c00388.

Supplementary tables and figures, HSQC data, experimental details, synthetic procedures, and characterization data (PDF)

AUTHOR INFORMATION

Corresponding Author

Brian C. Smith − *Department of Biochemistry, Program in Chemical Biology, Medical College of Wisconsin, Milwaukee, Wisconsin 53226, United States;* orcid.org/0000-0001-6330-2768; Phone: (414) 955-5669; Email: brismith@mcw.edu; Fax: (414) 955-6510

Authors

Daniel J. Sprague − *Department of Biochemistry, Program in Chemical Biology, Medical College of Wisconsin, Milwaukee, Wisconsin 53226, United States*

Anthony E. Getschman − *Department of Biochemistry, Program in Chemical Biology, Medical College of Wisconsin, Milwaukee, Wisconsin 53226, United States*

Tyler G. Fenske − *Department of Biochemistry, Program in Chemical Biology, Medical College of Wisconsin, Milwaukee, Wisconsin 53226, United States*

Brian F. Volkman − *Department of Biochemistry, Program in Chemical Biology, Medical College of Wisconsin, Milwaukee, Wisconsin 53226, United States;* orcid.org/0000-0002-6681-5179

Complete contact information is available at:
https://pubs.acs.org/10.1021/acsmedchemlett.1c00388

Author Contributions

D.J.S. performed chemical syntheses. A.E.G. performed NMR titrations. T.G.F. performed *in silico* docking. D.J.S. wrote the first draft of the manuscript. All of the authors worked on revisions and approved the final version of the manuscript.

Notes

The authors declare the following competing financial interest(s): B.F.V. has ownership interests in Protein Foundry, LLC and XLock Biosciences, LLC.

ABBREVIATIONS

GPCR, G-protein-coupled receptor; CXCL12, CXC motif chemokine 12; CXCR4, C-X-C chemokine receptor type 4; ACKR3, atypical chemokine receptor 3; PPI, protein−protein interaction; sY, sulfotyrosine; HSQC, heteronuclear single-quantum coherence spectroscopy; SAR, structure−activity relationship; NMR, nuclear magnetic resonance; Ph, phenyl; THF, tetrahydrofuran; Bn, benzyl; $Pd(dppf)_2Cl_2$, [1,1′-bis-(diphenylphosphino)ferrocene]dichloropalladium(II); Fe-$(acac)_3$, tris(acetylacetonato)iron(III); NMP, *N*-methyl-2-pyrrolidone; PhSH, thiophenol; Cy, cyclohexane; Me, methyl; LE, ligand efficiency; LLE, lipophilic ligand efficiency; HRMS, high-resolution mass spectrometry

REFERENCES

(1) Zlotnik, A.; Yoshie, O. The chemokine superfamily revisited. *Immunity* **2012**, *36*, 705−716.

(2) Le, Y.; Zhou, Y.; Iribarren, P.; Wang, J. Chemokines and chemokine receptors: their manifold roles in homeostasis and disease. *Cell. Mol. Immunol.* **2004**, *1*, 95−104.

(3) Nagasawa, T.; Hirota, S.; Tachibana, K.; Takakura, N.; Nishikawa, S.; Kitamura, Y.; Yoshida, N.; Kikutani, H.; Kishimoto, T. Defects of B-cell lymphopoiesis and bone-marrow myelopoiesis in mice lacking the CXC chemokine PBSF/SDF-1. *Nature* **1996**, *382*, 635−638.

(4) Chatterjee, S.; Behnam Azad, B.; Nimmagadda, S. Chapter Two - The Intricate Role of CXCR4 in Cancer. *Adv. Cancer Res.* **2014**, *124*, 31−82.

(5) Miao, M.; De Clercq, E.; Li, G. Clinical significance of chemokine receptor antagonists. *Expert Opin. Drug Metab. Toxicol.* **2020**, *16*, 11−30.

(6) Debnath, B.; Xu, S.; Grande, F.; Garofalo, A.; Neamati, N. Small molecule inhibitors of CXCR4. *Theranostics* **2013**, *3*, 47−75.

(7) De Clercq, E. Mozobil® (Plerixafor, AMD3100), 10 years after its approval by the US Food and Drug Administration. *Antivir. Chem. Chemother.* **2019**, *27*, 2040206619829382.

(8) Clinical trial no. NCT03154827.

(9) Abraham, M.; Klein, S.; Bulvik, B.; Wald, H.; Weiss, I. D.; Olam, D.; Weiss, L.; Beider, K.; Eizenberg, O.; Wald, O.; Galun, E.; Avigdor, A.; Benjamini, O.; Nagler, A.; Pereg, Y.; Tavor, S.; Peled, A. The CXCR4 inhibitor BL-8040 induces the apoptosis of AML blasts by downregulating ERK, BCL-2, MCL-1 and cyclin-D1 via altered miR-15a/16−1 expression. *Leukemia* **2017**, *31*, 2336−2346.

(10) Bockorny, B.; Semenisty, V.; Macarulla, T.; Borazanci, E.; Wolpin, B. M.; Stemmer, S. M.; Golan, T.; Geva, R.; Borad, M. J.; Pedersen, K. S.; Park, J. O.; Ramirez, R. A.; Abad, D. G.; Feliu, J.; Munoz, A.; Ponz-Sarvise, M.; Peled, A.; Lustig, T. M.; Bohana-Kashtan, O.; Shaw, S. M.; Sorani, E.; Chaney, M.; Kadosh, S.; Vainstein Haras, A.; Von Hoff, D. D.; Hidalgo, M. BL-8040, a CXCR4 antagonist, in combination with pembrolizumab and chemotherapy for pancreatic cancer: the COMBAT trial. *Nat. Med.* **2020**, *26*, 878−885.

(11) Clinical trial no. NCT03995108.

(12) McDermott, D. H.; Murphy, P. M. WHIM syndrome: Immunopathogenesis, treatment and cure strategies. *Immunol Rev.* **2019**, *287*, 91−102.

(13) Siciliano, S. J.; Rollins, T. E.; DeMartino, J.; Konteatis, Z.; Malkowitz, L.; Van Riper, G.; Bondy, S.; Rosen, H.; Springer, M. S. Two-site binding of C5a by its receptor: an alternative binding paradigm for G protein-coupled receptors. *Proc. Natl. Acad. Sci. U. S. A.* **1994**, *91*, 1214−1218.

(14) Sun, X.; Cheng, G.; Hao, M.; Zheng, J.; Zhou, X.; Zhang, J.; Taichman, R. S.; Pienta, K. J.; Wang, J. CXCL12/CXCR4/CXCR7 chemokine axis and cancer progression. *Cancer Metastasis Rev.* **2010**, *29*, 709−722.

(15) Hachet-Haas, M.; Balabanian, K.; Rohmer, F.; Pons, F.; Franchet, C.; Lecat, S.; Chow, K. Y.; Dagher, R.; Gizzi, P.; Didier, B.; Lagane, B.; Kellenberger, E.; Bonnet, D.; Baleux, F.; Haiech, J.; Parmentier, M.; Frossard, N.; Arenzana-Seisdedos, F.; Hibert, M.; Galzi, J. L. Small neutralizing molecules to inhibit actions of the chemokine CXCL12. *J. Biol. Chem.* **2008**, *283*, 23189−23199.

(16) Regenass, P.; Abboud, D.; Daubeuf, F.; Lehalle, C.; Gizzi, P.; Riche, S.; Hachet-Haas, M.; Rohmer, F.; Gasparik, V.; Boeglin, D.; Haiech, J.; Knehans, T.; Rognan, D.; Heissler, D.; Marsol, C.; Villa, P.; Galzi, J. L.; Hibert, M.; Frossard, N.; Bonnet, D. Discovery of a Locally and Orally Active CXCL12 Neutraligand (LIT-927) with Anti-inflammatory Effect in a Murine Model of Allergic Airway Hypereosinophilia. *J. Med. Chem.* **2018**, *61*, 7671−7686.

(17) Bordenave, J.; Thuillet, R.; Tu, L.; Phan, C.; Cumont, A.; Marsol, C.; Huertas, A.; Savale, L.; Hibert, M.; Galzi, J. L.; Bonnet, D.; Humbert, M.; Frossard, N.; Guignabert, C. Neutralization of CXCL12 attenuates established pulmonary hypertension in rats. *Cardiovasc. Res.* **2020**, *116*, 686−697.

(18) Hoellenriegel, J.; Zboralski, D.; Maasch, C.; Rosin, N. Y.; Wierda, W. G.; Keating, M. J.; Kruschinski, A.; Burger, J. A. The Spiegelmer NOX-A12, a novel CXCL12 inhibitor, interferes with chronic lymphocytic leukemia cell motility and causes chemo-sensitization. *Blood* **2014**, *123*, 1032−1039.

(19) Clinical trial no. NCT03168139.

(20) Smith, E. W.; Liu, Y.; Getschman, A. E.; Peterson, F. C.; Ziarek, J. J.; Li, R.; Volkman, B. F.; Chen, Y. Structural analysis of a novel small molecule ligand bound to the CXCL12 chemokine. *J. Med. Chem.* **2014**, *57*, 9693−9699.

(21) Veldkamp, C. T.; Ziarek, J. J.; Peterson, F. C.; Chen, Y.; Volkman, B. F. Targeting SDF-1/CXCL12 with a ligand that prevents activation of CXCR4 through structure-based drug design. *J. Am. Chem. Soc.* **2010**, *132*, 7242−7243.

(22) Irwin, J. J.; Shoichet, B. K. ZINC–a free database of commercially available compounds for virtual screening. *J. Chem. Inf. Model.* **2005**, *45*, 177−182.

(23) Smith, E. W.; Nevins, A. M.; Qiao, Z.; Liu, Y.; Getschman, A. E.; Vankayala, S. L.; Kemp, M. T.; Peterson, F. C.; Li, R.; Volkman, B. F.; Chen, Y. Structure-Based Identification of Novel Ligands Targeting Multiple Sites within a Chemokine-G-Protein-Coupled-Receptor Interface. *J. Med. Chem.* **2016**, *59*, 4342−4351.

(24) Getschman, A. E. Investigations into chemokine-receptor interactions for structure-guided ligand discovery. Doctoral dissertation, Medical College of Wisconsin, Milwaukee, WI, 2016.

(25) Williamson, M. P. Using chemical shift perturbation to characterise ligand binding. *Prog. Nucl. Magn. Reson. Spectrosc.* **2013**, *73*, 1−16.

(26) Yu, Z.; Li, P.; Merz, K. M., Jr Using Ligand-Induced Protein Chemical Shift Perturbations To Determine Protein-Ligand Structures. *Biochemistry* **2017**, *56*, 2349−2362.

(27) Pike, S. J.; Hutchinson, J. J.; Hunter, C. A. H-Bond Acceptor Parameters for Anions. *J. Am. Chem. Soc.* **2017**, *139*, 6700−6706.

(28) Zhang, Y.; Reeder, E. K.; Keaton, R. J.; Sita, L. R. Goldilocks Effect of a Distal Substituent on Living Ziegler-Natta Polymerization Activity and Stereoselectivity within a Class of Zirconium Amidinate-Based Initiators. *Organometallics* **2004**, *23*, 3512−3520.

(29) Dai, C.; Fu, G. C. The first general method for palladium-catalyzed Negishi cross-coupling of aryl and vinyl chlorides: use of commercially available Pd(P(t-Bu)$_3$)$_2$ as a catalyst. *J. Am. Chem. Soc.* **2001**, *123*, 2719−2724.

(30) Furstner, A.; Leitner, A.; Mendez, M.; Krause, H. Iron-catalyzed cross-coupling reactions. *J. Am. Chem. Soc.* **2002**, *124*, 13856−13863.

(31) Ma, J. C.; Dougherty, D. A. The Cation-π Interaction. *Chem. Rev.* **1997**, *97*, 1303−1324.

(32) Gallivan, J. P.; Dougherty, D. A. Cation-π interactions in structural biology. *Proc. Natl. Acad. Sci. U. S. A.* **1999**, *96*, 9459−9464.

(33) Zacharias, N.; Dougherty, D. A. Cation-π interactions in ligand recognition and catalysis. *Trends Pharmacol. Sci.* **2002**, *23*, 281−287.

(34) Crowley, P. B.; Golovin, A. Cation-π interactions in protein-protein interfaces. *Proteins: Struct., Funct., Genet.* **2005**, *59*, 231−239.

(35) Flocco, M. M.; Mowbray, S. L. Planar stacking interactions of arginine and aromatic side-chains in proteins. *J. Mol. Biol.* **1994**, *235*, 709−717.

(36) Anderson, M. A.; Ogbay, B.; Arimoto, R.; Sha, W.; Kisselev, O. G.; Cistola, D. P.; Marshall, G. R. Relative strength of cation-π vs salt-bridge interactions: the G$_t\alpha$(340−350) peptide/rhodopsin system. *J. Am. Chem. Soc.* **2006**, *128*, 7531−7541.

(37) Stepan, A. F.; Subramanyam, C.; Efremov, I. V.; Dutra, J. K.; O'Sullivan, T. J.; DiRico, K. J.; McDonald, W. S.; Won, A.; Dorff, P. H.; Nolan, C. E.; Becker, S. L.; Pustilnik, L. R.; Riddell, D. R.; Kauffman, G. W.; Kormos, B. L.; Zhang, L.; Lu, Y.; Capetta, S. H.; Green, M. E.; Karki, K.; Sibley, E.; Atchison, K. P.; Hallgren, A. J.; Oborski, C. E.; Robshaw, A. E.; Sneed, B.; O'Donnell, C. J. Application of the bicyclo[1.1.1]pentane motif as a nonclassical phenyl ring bioisostere in the design of a potent and orally active gamma-secretase inhibitor. *J. Med. Chem.* **2012**, *55*, 3414−3424.

(38) Leeson, P. D.; Springthorpe, B. The influence of drug-like concepts on decision-making in medicinal chemistry. *Nat. Rev. Drug Discovery* **2007**, *6*, 881−890.

(39) See Table S1 for a list of parameters of other ligands.